

A TEST FOR RADIAL MIXING USING LOCAL STAR SAMPLES

JINCHENG YU

Key Laboratory for Research in Galaxies and Cosmology, Shanghai Astronomical Observatory,
Chinese Academy of Sciences, 80 Nandan Road, Shanghai 200030, China
Graduate University of the Chinese Academy of Sciences, 19A Yuquanlu, Beijing 100049, China
yujc@shao.ac.cn

J. A. SELLWOOD AND CARLTON PRYOR

Department of Physics and Astronomy, Rutgers University,
136 Frelinghuysen Road, Piscataway, NJ 08854
sellwood,pryor@physics.rutgers.edu

LI CHEN AND JINLIANG HOU

Key Laboratory for Research in Galaxies and Cosmology, Shanghai Astronomical Observatory, Chinese
Academy of Sciences, 80 Nandan Road, Shanghai 200030, China
chenli,houjl@shao.ac.cn

Accepted to appear in ApJ May 29, 2012, first submitted Sep 30, 2011

ABSTRACT

We use samples of local main-sequence stars to show that the radial gradient of [Fe/H] in the thin disk of the Milky Way decreases with mean effective stellar temperature. Many of these stars are visiting the solar neighborhood from the inner and outer Galaxy. We use the angular momentum of each star about the Galactic center to determine the guiding center radius and to eliminate the effects of epicyclic motion, which would otherwise blur the estimated gradients. We interpret the effective temperature as a proxy for mean age, and conclude that the decreasing gradient is consistent with the predictions of radial mixing due to transient spiral patterns. We find some evidence that the trend of decreasing gradient with increasing mean age breaks to a constant gradient for samples of stars whose main-sequence life-times exceed the likely age of the thin disk.

Subject headings: Stars: abundances — galaxies: kinematics and dynamics

1. INTRODUCTION

A radial abundance gradient in the Milky Way disk today is well-established from analyses of the interstellar medium (Shaver *et al.* 1983; Balsa *et al.* 2011). Metal abundances are believed to increase over time and most chemical evolution models (*e.g.*, Boissier & Prantzos 1999; Hou *et al.* 2000; Chiappini *et al.* 2001; Naab & Ostriker 2006; Fu *et al.* 2009) predict that a radial abundance gradient is created early and may even have been steeper in the past. This picture is consistent with “inside-out” disk formation, in which the stellar population at increasing radii is younger and more metal poor (*e.g.* de Jong 1999; Muñoz-Mateos *et al.* 2007).

The chemical composition of a star is that of the cloud of gas from which it formed. Abundance gradients are therefore also observed in the disk of the Milky Way in stars (Nordström *et al.* 2004; Haywood 2008; Luck *et al.* 2011; Schlesinger *et al.* 2011), in planetary nebulae (Maciel *et al.* 2007; Stanghellini & Haywood 2010), and in open star clusters (Friel *et al.* 2002; Chen *et al.* 2003). While all agree that abundances in the thin disk decrease outwards, the precise slope differs from sample to sample and element measured.

The orbits of disk stars generally become more eccentric over time (Wielen 1977; Holmberg *et al.* 2009; Aumer & Binney 2009), which “blurs” measurements of the metallicity gradient when the instantaneous radii of older stars are used. Eccentric motion of any amplitude, projected to the mid-plane of an axisymmetric potential, can be described as a retrograde epicycle about a guiding center that orbits at a constant angular rate (Binney & Tremaine 2008). The guiding center, or home, radius of a disk star is

directly related to the z -component of the angular momentum, L_z , about the Galactic center and, since angular momentum is conserved, can be determined from any point around the epicycle. Thus measurement of the angular momenta of stars allows us to eliminate the blurring effects of epicyclic motions and simplifies the interpretation of metallicity gradients. Nordström *et al.* (2004) used the mean Galacto-centric radius for the same reason, which requires integrating the orbit in some adopted potential – angular momentum is more direct.

In the absence of radial mixing, chemical evolution models in which the metallicity of the ISM increases at each radius over time would predict a tight correlation between the metallicity and age for stars of a given home radius. This prediction is not supported by the data, and the metallicity distribution of all but the youngest stars shows a broad distribution (Edvardsson *et al.* 1993; Nordström *et al.* 2004), which persists even after correcting for epicyclic blurring (Haywood 2008).

Sellwood & Binney (2002) argued that stars in a disk galaxy are shuffled in radius over time by the effects of transient spiral arms. They showed that a star near the corotation resonance of a spiral could gain or lose enough angular momentum for its home radius to change by up to 2 kpc, leaving the star at its new mean galacto-centric distance with no increase in its epicyclic amplitude. The resulting radial mixing is described as “churning” and their result has been confirmed and extended (Roškar *et al.* 2008a,b; Loebman *et al.* 2011; Minchev *et al.* 2011; Bird *et al.* 2012; Solway *et al.* 2012). The broad spread of metallicities among stars having common ages and home radii today is then naturally explained as reflecting the past gra-

dient of metallicity of the ISM at their various birth radii. Schönrich & Binney (2009) provide a model for chemical evolution of the Milky Way that was the first to include radial mixing. Loebman *et al.* (2011) find good agreement between the predictions of their simulations, that manifest substantial radial mixing, with the metallicity distribution of stars from the SDSS (Ivezić *et al.* 2008); Lee *et al.* (2011) find other evidence supporting radial migration.

An additional consequence of radial mixing, or churning, is that the radial metallicity gradient of a generation of stars is gradually flattened over time. Nordström *et al.* (2004) and Haywood (2008), from local stars suggest that the gradient may become shallower with increasing age. Casagrande *et al.* (2011) report little evolution of the radial metallicity gradient over the past ~ 5 Gyr, using infrared magnitudes and improved models to revise the age estimates for the stars in the Nordström *et al.* (2004) sample. Estimating the age of an individual star (see Soderblom 2010, for a recent review) is a delicate art and the results even for well-observed main-sequence stars can be contentious (*e.g.* Reid *et al.* 2007; Holmberg *et al.* 2007). Furthermore, the evidence from star clusters (Friel *et al.* 2002; Chen *et al.* 2003) suggests that the radial metallicity gradient may steepen with age, in line with inside-out models of galaxy formation. Maciel *et al.* (2007), from a study of planetary nebulae abundance data, also find evidence for a steeper gradient among their older objects, although Stanghellini & Haywood (2010) reach the opposite conclusion that older PNe show a shallower gradient. We comment on these apparently conflicting results in §4.2.

Here we study the age-dependence of the metallicity gradient using a sample of stars in the solar neighborhood. Instead of estimating ages of individual stars, we adopt the effective temperature of a collection of main sequence stars as a proxy for their mean age, in the same manner that Aumer & Binney (2009) used color. Since the main-sequence lifetime of a star is shorter for hotter stars, the mean ages of main sequence disk stars grouped by effective temperature must be lower for the hotter groups. (Of course, this argument requires the reasonable assumptions that stars have been forming with an approximately constant IMF and at a roughly uniform rate over the lifetime of the Milky Way disk.) The trend of increasing mean age with decreasing temperature must change to a constant at the point at which the main-sequence lifetimes of stars exceed the age of the disk. Note that the main-sequence turn-off for stars of age 10 Gyr occurs for $5\,500 \lesssim T_{\text{eff}} \lesssim 6\,000$ K over the range $0.4 \gtrsim [\text{Fe}/\text{H}] \gtrsim -0.5$ (Demarque *et al.* 2004).

As explained above, we eliminate epicyclic blurring by estimating the specific angular momentum of each star, which requires knowledge of its full 6D phase space coordinates: *i.e.* distance and proper motion, as well as radial velocity and sky position. A radial velocity can be measured spectroscopically at any distance, but a reliable distance can be obtained only for nearby stars. Furthermore, distance uncertainties factor into velocity components in the sky plane adding to the desirability of restricting attention to stars close to the Sun. Also, by focusing on nearby stars, any variations in L_z across our sampling volume due to possible departures from axisymmetry in the

Galactic potential will be negligible.

A benefit of stellar epicycle excursions is that they bring stars to the solar neighborhood. Thus a sample of very local stars will span a significant range of specific angular momenta and, therefore, home radii.

In this paper, we assemble a sample of local, main-sequence stars having estimated effective temperatures, metallicities and full space motions. We draw these stars from three sources as described in the next section.

2. STAR SAMPLES

2.1. Geneva-Copenhagen sample

The Geneva-Copenhagen survey of nearby stars (Nordström *et al.* 2004) used *Hipparcos* positions and proper motions, supplemented by spectroscopic observations, to construct a homogeneous sample of nearby mostly F and G dwarf stars. We employ their updated catalog (Holmberg *et al.* 2009) that uses their revised temperature calibration and the improved astrometry from the reanalysis of *Hipparcos* data by van Leeuwen (2007). This monumental effort has resulted in a large sample of stars in the solar neighborhood with distances and full space motions. Holmberg *et al.* (2009) do not supply individual uncertainties for each velocity, but assert that they are believed accurate to 1.5 km s^{-1} , with the greatest contribution coming from distance uncertainties.

The machine readable table of 16 682 stars made available by Holmberg *et al.* (2009) includes sky positions, distances, and the (U, V, W) components of the star's motion relative to the Sun in Galactic coordinates.¹ We discard those having no distance, no (U, V, W) velocities, or no estimate of T_{eff} . We do not use the disputed age estimates (*e.g.* Reid *et al.* 2007; Holmberg *et al.* 2007) in the present paper. We correct for Solar motion relative to the local standard of rest (LSR) by adding $(U, V, W)_{\odot} = (11.10, 12.24, 7.25) \text{ km s}^{-1}$ (Schönrich *et al.* 2010) to the tabulated velocities.

Nordström *et al.* (2004) note that they obtained $[\text{Fe}/\text{H}] \gtrsim 0.4$ for a small number of stars, though none is within 40 pc of the Sun. Furthermore, these high values are found only for stars with $T_{\text{eff}} \gtrsim 6200$ K. They argue that the coincidence of high T_{eff} and $[\text{Fe}/\text{H}]$, together with other information, suggests that the extinction to these stars has been overestimated. We therefore discard a further 29 stars having $[\text{Fe}/\text{H}] > 0.4$.

In order to select nearby disk stars, we further restrict the sample to stars whose best estimate of the distance is within 500 pc, $|U|, |V| < 80 \text{ km s}^{-1}$, and retain only those having an energy of vertical motion about the Galactic mid-plane, $E_z = 0.5(z^2\nu^2 + W^2) < 392 \text{ (km s}^{-1}\text{)}^2$, with the vertical frequency $\nu = 0.07 \text{ km s}^{-1} \text{ pc}^{-1}$ (Binney & Tremaine 2008), giving them a maximum vertical excursion of ± 400 pc. Thus we select only stars that have a high probability of being thin disk stars, in the same spirit as Bensby *et al.* (2003), but not in exactly the same manner² (see §4 for further discussion of selection effects). Our final

¹ These Cartesian velocity components are oriented such that U is towards the Galactic centre, V is in the direction of Galactic rotation, and W is towards the north Galactic pole.

² Adopting their selection criterion for thin disk stars, changes the number of selected stars by a few hundred, but our conclusions are unaffected by this marginal revision.

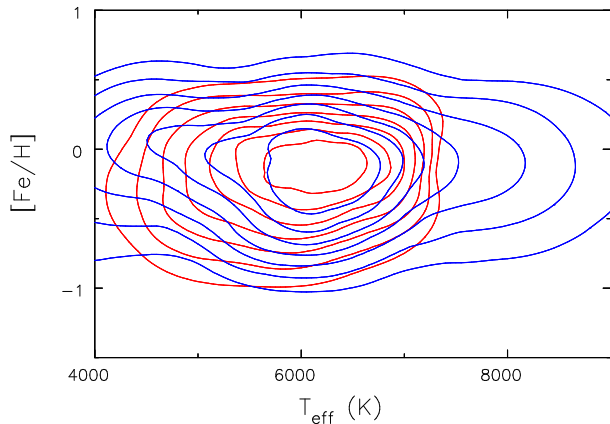


FIG. 1.— The densities of stars in the space of T_{eff} and $[\text{Fe}/\text{H}]$ in our selected GCS (red) and RAVE (blue) subsamples.

sample contains 11 877 stars that we use in this analysis.

The median distance of the selected stars is 75 pc and the sample within 40 pc of the Sun is believed to be near complete. We adopt $R_0 = 8$ kpc, the circular speed of the LSR to be $V_0 = 220$ km s $^{-1}$, and compute the Galactocentric angular momentum, L_z , using the in-plane distance of the star from the Sun and the peculiar velocities (U, V) corrected for the Sun’s motion.

The red contours in Fig. 1 show the distribution of the selected GCS stars in the space of T_{eff} and $[\text{Fe}/\text{H}]$. The range of T_{eff} indicates that the sample extends outside the spectral types F and G, reflecting the selection criteria described by Nordström *et al.* (2004). These authors estimate uncertainties of $\lesssim 0.1$ in $[\text{Fe}/\text{H}]$ and 94 K in T_{eff} .

Casagrande *et al.* (2011) present a recalibration of T_{eff} and $[\text{Fe}/\text{H}]$ for the GCS stars that folds in the infrared flux from a star. They obtain slightly higher values for T_{eff} and $[\text{Fe}/\text{H}]$ than those derived by Holmberg *et al.* (2009) and they too attempt to assign ages for the individual stars. The additional information used by Casagrande *et al.* (2011) should lead to improved values for the derived quantities, but they claim reliable results for fewer than half the GCS stars (their *irfm* sample) and for none of the cooler stars. We therefore continue to use the calibration for the whole GCS sample by Holmberg *et al.* (2009).

2.2. RAVE sample

The RAVE survey (Steinmetz *et al.* 2006) plans to measure the heliocentric radial velocities and stellar parameters for about a million stars in the southern sky having apparent magnitudes in the range $9 < m_I < 12$; the first 77 461 are available in the third data release (Siebert *et al.* 2011). The typical uncertainty in the radial velocity is < 2 km s $^{-1}$, but the distance to most stars has to be judged photometrically and most proper motions are from ground-based data. Thus three of the phase space coordinates for each star are of much lower quality than are those in the GCS, although this weakness will be compensated by a much larger sample size when the survey is complete.

We have downloaded the on-line table of the third data release from the RAVE website and selected a subset of stars for analysis.³ We estimate distances to these stars

³ The paper by Coşkunoglu *et al.* (2011) presenting an analysis of

by fitting to the Yonsei-Yale isochrones (Demarque *et al.* 2004) using a method related to that described by Breddels *et al.* (2010, see also Burnett *et al.* 2011 for an alternative method). We adopt many of their selection criteria: we require the spectral signal-to-noise parameter $S2N > 20$ with a blank spectral warning flag field; the parameters $[\text{M}/\text{H}]$, $\log(g)$, and T_{eff} to be determined; and the stars to have J and K_s magnitudes from 2MASS with no warning flags about the identification of the star or the 2MASS photometry. Unlike those authors, however, we have kept stars with $b < 25^\circ$ on the grounds that extinction for the nearby stars that interest us will not be large enough in the near IR to severely bias our distance estimates. As we are here interested only in nearby main-sequence stars that are members of the disk population, we also make preliminary cuts to eliminate stars with $\log(g) < 4$, $T_{\text{eff}} > 10^4$ K, and with $|v_r| > 120$ km s $^{-1}$. We have treated the tabulated $[\text{M}/\text{H}]$ as equivalent to $[\text{Fe}/\text{H}]$ since the corrections (Zwitter *et al.* 2008) are generally within the uncertainties. We also show in §2.3 that the $[\text{M}/\text{H}]$ values for RAVE stars agree with the $[\text{Fe}/\text{H}]$ values for the stars in common with the GCS.

We estimate the absolute J magnitude of each selected star by matching the estimated $[\text{Fe}/\text{H}]$, $\log(g)$, T_{eff} , and J- K_s color to values in the isochrone tables for stars of all ages and all values of $[\alpha/\text{Fe}]$, rejecting a few more stars for which the best match $\chi^2 > 6$. We consider the closest match in the tables to the given input parameters to yield the best estimate of the absolute magnitude from which we estimate a photometric distance using the apparent J-band magnitude.⁴ We save the values of $[\text{Fe}/\text{H}]$, $\log(g)$, T_{eff} , and J- K_s color of the closest matching model star in the isochrone table; Monte-Carlo variation of the stellar parameters about this saved set of values suggests that distances have a fractional precision of 30% – 50%, with some larger uncertainties.

We use the proper motions in equatorial coordinates tabulated in RAVE, mostly from Tycho-2 (Høg *et al.* 2000),⁵ which we then combine with the radial velocity and position to determine the heliocentric velocity in Galactic components (U, V, W) (Johnson & Soderblom 1987; Piatek *et al.* 2002). We estimate uncertainties in these velocities from 500 Monte Carlo re-selections of all the stellar parameters that affect the distance estimate, adopting $\sigma(J) = 0.03$ mag, $\sigma(J - K_s) = 0.042$ mag, $\sigma(T_{\text{eff}}) = 300$ K, $\sigma(\log g) = 0.3$ dex, and $\sigma([\text{Fe}/\text{H}]) = 0.25$ dex (Breddels *et al.* 2010), as well as the tabulated radial velocity and proper motion uncertainties.

We exclude stars more distant than 500 pc, correct the space velocities for solar motion and apply the same restrictions as for the GCS sample to select only those with a high probability of being thin disk stars.

Fig. 2 shows histograms of distances and of uncertainties in L_z for the 9, 803 remaining stars. The median distance

the radial abundance gradient from these same stars appeared while this paper was in review.

⁴ Zwitter *et al.* (2010) describe a similar method, but define a “most likely” estimate of the absolute magnitude that differs from our “best” estimate. The difference is likely to be well within the uncertainties for the main-sequence stars considered here.

⁵ We have not used the newly available proper motions from the fourth release of the Southern Proper Motion Catalog (Girard *et al.* 2011)

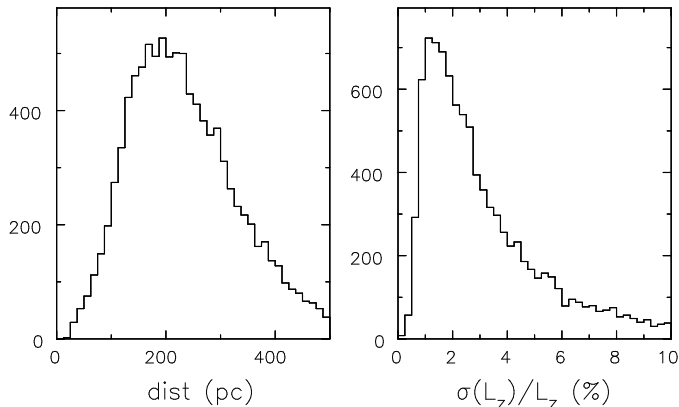


FIG. 2.— Histograms of distances and L_z uncertainties for the selected sample of 9803 RAVE stars.

is 220 pc from the Sun and uncertainties in L_z are generally smaller than 5%.

The blue contours in Fig. 1 show the distribution of selected RAVE stars. The distribution in $[\text{Fe}/\text{H}]$ values is slightly broader than for the GCS stars, reflecting in part at least the lower precision of the spectra. However, the rms scatter in $[\text{Fe}/\text{H}]$ appears to be ~ 0.2 , suggesting the uncertainty of 0.25 estimated by Siebert *et al.* (2011) is somewhat pessimistic for this sub-sample of main-sequence stars. These authors also suggest uncertainties of 300 K in their estimates of T_{eff} , and the broader range of T_{eff} than in the GCS sample is therefore real.

2.3. Stars in common

The overlap between the GCS and RAVE samples of stars is quite small but, of those we have selected, precisely 100 stars are positionally coincident. This small degree of overlap allows us to compare the spectral parameters, T_{eff} , $[\text{Fe}/\text{H}]$, and radial velocity (v_r), derived separately by the two teams from their independent spectra.

We find that differences in the estimated v_r for the same stars average just 0.32 km s^{-1} higher in RAVE than in GCS, with an rms scatter about this mean of only 2.3 km s^{-1} . Similarly, differences in T_{eff} have a mean of 203 K, again higher in RAVE than in GCS, with an rms scatter about the mean of 202 K. Finally, the mean difference in $[\text{Fe}/\text{H}]$ is 0.057, lower in RAVE than in GCS, with an rms scatter of 0.18. We have looked in vain for systematic variations of these differences, which appear to be consistent with random scatter.

Thus all three spectral parameters agree between the independent measures to an accuracy that is significantly better than expected from the quoted uncertainties, indicating that both teams have been very careful with their calibrations and conservative with their uncertainty estimates.

2.4. M-dwarf sample

The SDSS (York *et al.* 2000) and Segue2 (Yanny *et al.* 2009) surveys are complete, but sample fainter stars than RAVE (the magnitude range for Segue2 was $14.0 < g < 20.3$) that are therefore generally more distant. Since the Sloan spectral parameters pipeline (Lee *et al.* 2008) does

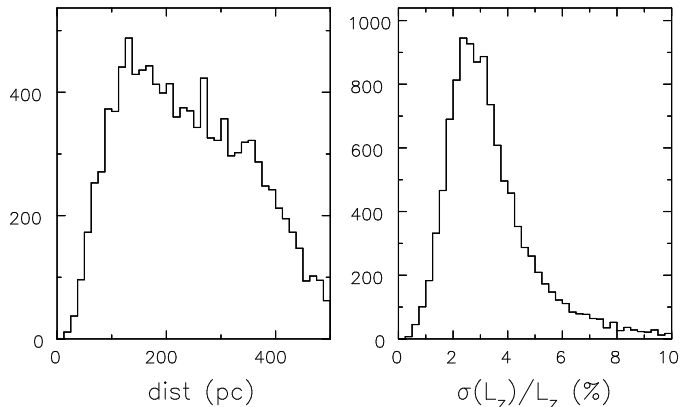


FIG. 3.— Histograms of distances and L_z uncertainties for the selected sample of 11 022 M-dwarf stars.

not attempt to fit stars with $T_{\text{eff}} \lesssim 4500 \text{ K}$, almost all main sequence stars with estimated parameters in SDSS DR8 are more distant than 500 pc.

Fortunately, West *et al.* (2011) provided a catalog of 70 841 M-dwarfs from SDSS DR7. Their table provides a photometric estimate of the distance to each star, as well as a spectroscopic radial velocity, and proper motion from USNO-B/SDSS catalog (Munn *et al.* 2004, 2008). They suggest that distance uncertainties are typically about 20% and uncertainties in radial velocity are $7\text{--}10 \text{ km s}^{-1}$. None of these stars are in RAVE (because they are in different parts of the sky) and all are much cooler than the GCS stars.

As West *et al.* (2011) recommend, we selected stars with the “goodPM” and “goodPhot” flags set to ‘true’, and the “WDM” flag set to ‘false’ to eliminate possible binaries with a white dwarf companion, which reduces the sample to 39 151 stars. We further excluded stars having no radial velocity as well as those with no distance estimate or for which the estimated distance exceeded 500 pc. As for the GCS and RAVE stars, we correct the space velocities for solar motion and apply the same restrictions to select only those with a high probability of being thin disk stars, leaving us with a final sample of 11 022 stars.

We estimated uncertainties in the velocity components, (U, V, W) by combining the 20% distance uncertainty, a 10 km s^{-1} uncertainty in the radial velocity, and the proper motion uncertainties. The distribution of distances and fractional L_z uncertainties is shown in Fig. 3; many of these intrinsically faint stars lie within 200 pc and, again, angular momentum uncertainties are typically $\lesssim 5\%$.

As estimates of T_{eff} or $[\text{Fe}/\text{H}]$ are not easily derived from low resolution spectra of such cool stars, West *et al.* (2011) do not attempt to provide these quantities in their catalog. Instead, they provide spectral sub-class, which can be related to T_{eff} , and a titanium oxide index, ζ_{TiO} , which is believed to be an indicator of metallicity.

3. RESULTS

3.1. GCS and RAVE stars

Figs. 4 & 5 show the metallicity *vs.* angular momentum of GCS and RAVE stars each separately binned into various temperature ranges. The bins are chosen so as to have

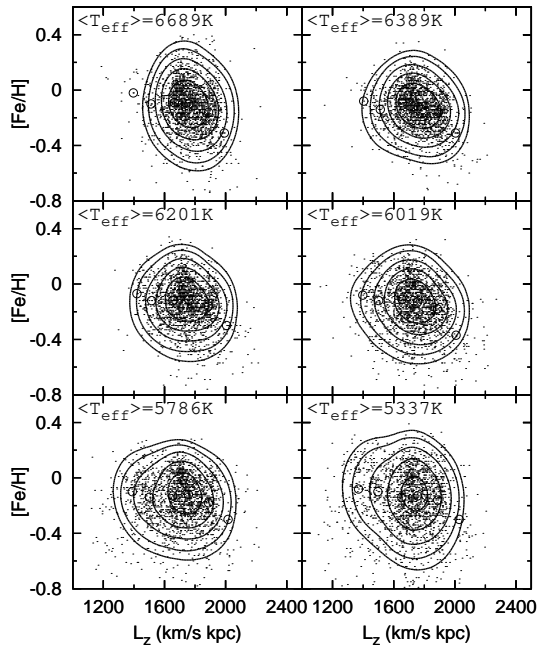


FIG. 4.— The distributions of GCS stars in the space of L_z and $[\text{Fe}/\text{H}]$ when grouped by effective temperature. The temperature bins were chosen to contain equal numbers of stars and the average temperature of the stars in each bin is given. The large open circles, which are purely to illustrate the trends, show the median $[\text{Fe}/\text{H}]$ for stars with $1300 < L_z < 2100$ divided into six bins in each panel. The unit of angular momentum is $\text{km s}^{-1} \text{kpc}$.

equal numbers of stars, and the average T_{eff} of the stars in each panel is shown. The density of points in each panel is indicated by the contours.

If the rotation curve of the Milky Way were flat at a constant circular speed of 220 km s^{-1} , then stars with $L_z = 1210 \text{ km s}^{-1} \text{kpc}$ would have home radii of 5.5 kpc, while the home radii of those with $L_z = 2200 \text{ km s}^{-1} \text{kpc}$ would be 10 kpc. (Note that these numerical values will simply scale with our choices of R_0 and V_0 .) Thus, although the stars in our sample are passing close to the Sun right now, many are visiting from quite far afield.

A number of trends can be seen: The spread in L_z is greater for the cooler stars, reflecting the fact that the higher velocity dispersions of older stars allows stars having a wider range of L_z to visit the solar neighborhood. The rms scatter in $[\text{Fe}/\text{H}]$ is in the range $0.19 \lesssim \sigma \lesssim 0.23$ for the RAVE stars in each panel, which is less than the nominal uncertainty, as noted in §2.2. The spread in $[\text{Fe}/\text{H}]$ for the GCS stars is generally smaller, rising from 0.14 in the second panel to 0.21 for the coolest stars. The spread for the hottest GCS stars (0.16) is anomalously high, due to incomplete removal of stars that were over-corrected for reddening, as noted in §2.1. While the large spread in $[\text{Fe}/\text{H}]$ is partly due to uncertainties and partly real, each panel has a weak declining trend of metallicity with increasing L_z that reflects the metallicity gradient in the Galaxy. We have added the open circles, which show the variation of the median in bins of L_z in each panel, simply to make this last trend more clearly visible.

3.2. Trend in gradient

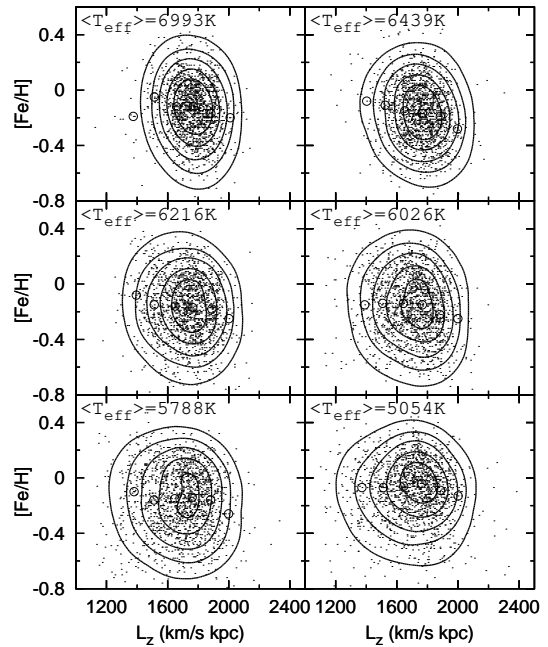


FIG. 5.— Same as Fig. 4, but for the RAVE sample.

We adopt Theil’s non-parametric method (Hollander & Wolfe 1999) to quantify the metallicity gradient in each panel, which we plot as filled symbols in Fig. 6, with the dashed error bars showing the 95% confidence limits. This method returns the median slope between every pair of points in the sample with the confidence limits being determined by the range of the pairwise values. We have converted the gradient with angular momentum to the more usual dex per kpc by multiplying by our adopted circular speed $V_0 = 220 \text{ km s}^{-1}$. Our abundance gradient estimates therefore assume only a locally flat rotation curve and a distance scale set by adopting $R_0 = 8 \text{ kpc}$.

While these estimates of the metallicity gradient are derived from stars that happen to be close to the Sun at the present time, the sample includes stars from a broad range of home radii, as noted above. Stars whose ages greatly exceed the radial epicycle period, $\sim 170 \text{ Myr}$ at the solar radius, should be uniformly distributed in radial phase around their epicycles. Thus both the spread in metallicities of the stars in our sample and the gradient we measure are characteristic of the stars at their home radii, and our estimates of the metallicity gradient are based on a radial range of several kiloparsec.

The apparent flattening of the metallicity gradient with decreasing T_{eff} is suggested by the RAVE stars (left panel of Fig. 6) and is more convincing in the better-quality data of the GCS sample (right panel). As this is our main result, we use Monte-Carlo simulations to check whether the uncertainties in the slopes are small enough to justify our claim of a trend. We generate 100 new samples, by randomly resampling stars, adding normally distributed values to T_{eff} , $[\text{Fe}/\text{H}]$, and L_z to simulate measurement errors. The size of the errors are determined by the appropriate uncertainties from each survey as described above or, for the L_z values of the RAVE stars, by propagating

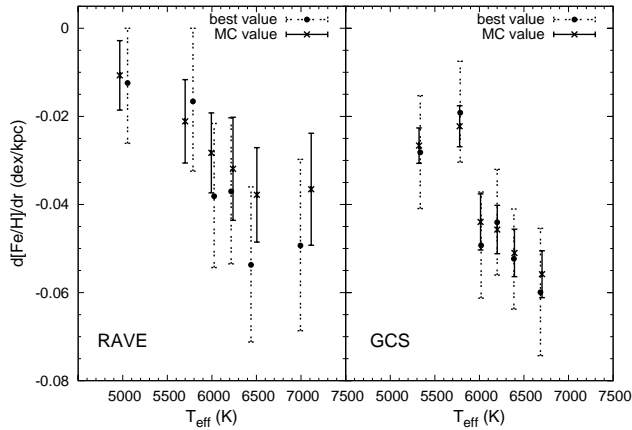


FIG. 6.— The metallicity gradient, $d[\text{Fe}/\text{H}]/dL_z$ estimated from the GCS sample shown in Fig. 4 (right panel), and from the RAVE sample in Fig. 5 (left panel). The filled symbols show the best estimate from Theil’s algorithm, with 95% confidence limits (dashed), the crosses with solid error bars show the standard errors derived from a Monte Carlo simulation with the adopted uncertainties.

our own estimates of the distance, proper motion and radial velocity uncertainties. We divide each sample into equal numbers of stars in successive bins of T_{eff} and compute the slopes. The means and standard errors of these re-estimates are also shown by the crosses and solid error bars in Fig. 6. Note that the solid error bars from our Monte-Carlo simulations indicate the $1-\sigma$ dispersion, whereas the dashed error bars from the Theil algorithm show the 95% confidence interval; the two independent estimates are therefore consistent, and the flattening of the slope with decreasing T_{eff} seems to be confirmed. Note also that the somewhat shallower trend in the Monte-Carlo re-estimates from the RAVE data is expected, since resampling the data in this manner inserts additional uncertainties over and above those already present in the data, which inevitably weakens a trend. This effect is more marked in the RAVE sample because uncertainties in their data are larger.

It also occurred to us that the change of slope could perhaps be a systematic effect due to the above-noted increasing spread in L_z with decreasing T_{eff} – *i.e.*, the greater spread in L_z could simply make the fitted slope appear shallower, while in fact the data may be consistent with a constant slope. We tested for this possibility by creating some pseudo star samples that adopt a linear relation between $[\text{Fe}/\text{H}]$ and L_z that is the same for all the stars in either the RAVE or the GCS sample, irrespective of their temperature, which is the null hypothesis that we argue Fig. 6 disproves. For each star in the sample, we use the measured L_z to assign a new $[\text{Fe}/\text{H}]$ from a Gaussian distribution about the mean from the adopted trend with a dispersion equal to that about the linear regression line for the entire sample. We then bin this pseudo-sample by T_{eff} as before and test whether the cooler stars, that have the larger spread in L_z , have a shallower apparent slope. With 500 realizations for each of the GCS and RAVE samples, we confirmed that we recover the original input slope in every bin. The absence of any systematic trend with T_{eff}

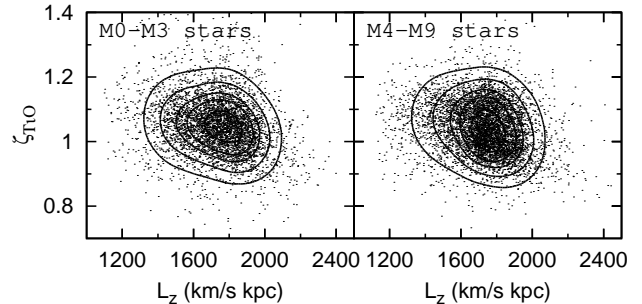


FIG. 7.— TiO index, ζ_{TiO} vs. angular momentum for the M-dwarf sample, divided by spectral sub-type into two roughly equally numerous groups.

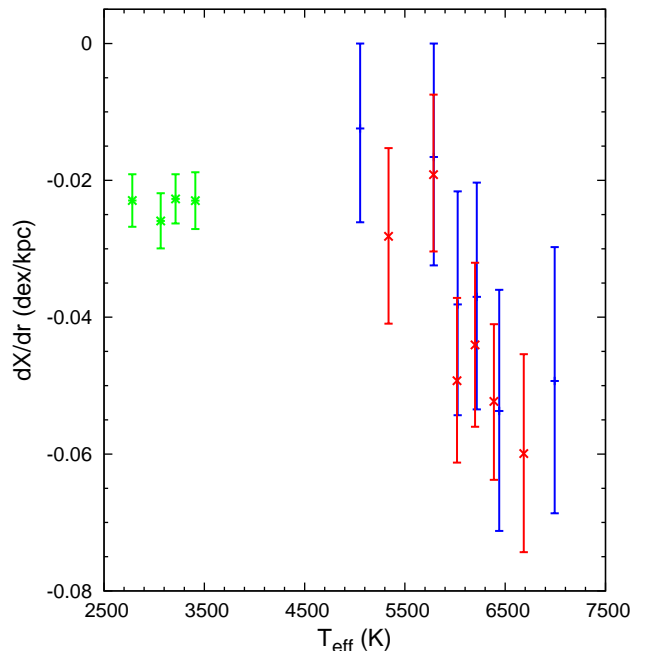


FIG. 8.— The estimated metallicity gradient $d[\text{Fe}/\text{H}]/dL_z$ from the GCS stars (red) and from the RAVE stars (blue) reproduced from Fig. 6. The green points show $d\zeta_{\text{TiO}}/dL_z$ from the M-dwarf stars in Fig. 7 further subdivided by spectral sub-class. The error bars show 95% confidence limits from Theil’s algorithm.

in this test increases our confidence that the trend we find in the data in Fig. 6 is real.

Furthermore, both samples also hint at a break in the trend with temperature around $T_{\text{eff}} \lesssim 6000$ K, although these points alone are also consistent with a uniform trend. In order to find extra evidence for this possible break of slope, we attempt to include the M-dwarf stars into our analysis.

3.3. M-dwarf sample

Fig. 7 shows the distribution of L_z and ζ_{TiO} for the M-dwarf stars separated into two groups by spectral class. This metallicity indicator again has a noticeable gradient with L_z .

As for the hotter stars, we have used Theil’s algorithm

to estimate the gradient $d\zeta_{\text{TiO}}/dL_z$, dividing the M-dwarf sample into four groups by stellar sub-class, and plot the results in green in Fig. 8. (The abscissae were determined from the relation $T_{\text{eff}} = 3700 - 150S$ K, where S is the spectral sub-class, fitted by eye to the compilation by Reylé *et al.* (2011).) The M-dwarfs have a constant metallicity gradient that appears independent of T_{eff} .

Because they are measured from a different quantity, the values of $d\zeta_{\text{TiO}}/dL_z$ cannot be compared directly with those of $d[\text{Fe}/\text{H}]/dL_z$ from the hotter stars, shown in red and blue. We tried using the empirical relation between ζ_{TiO} and $[\text{Fe}/\text{H}]$ suggested by Woolf *et al.* (2009), but many $[\text{Fe}/\text{H}]$ values required an extrapolation beyond the range calibrated by their study, and the resulting mean $[\text{Fe}/\text{H}]$ is unreasonably high. Thus we lack a direct basis to relate the green points in Fig. 8 to the others.

However, we note that if ζ_{TiO} is proportional to $[\text{Fe}/\text{H}]$, the gradient $d[\text{Fe}/\text{H}]/dL_z$ will scale with $d\zeta_{\text{TiO}}/dL_z$, and we would merely need to shift the green points vertically by some fixed factor to bring them onto the same scale. Since an anti-correlation between ζ_{TiO} and $[\text{Fe}/\text{H}]$ seems unlikely, the green points probably could not be shifted above $d[\text{Fe}/\text{H}]/dL_z = 0$. Thus the data from the M-dwarf stars do seem to confirm that the decreasing trend of metallicity gradient with T_{eff} among the hotter stars really does break to no trend around $T_{\text{eff}} \lesssim 6000$ K, *i.e.* for stars whose main-sequence lifetimes are $\sim 10^{10}$ yr.

4. DISCUSSION

Many authors (*e.g.* Lee *et al.* 2011; Casagrande *et al.* 2011; Coşkunoğlu *et al.* 2011) express concerns that estimates of the metallicity gradient from a sample of stars depend upon the adopted selection criteria. This is because metallicity is a function of age and, relative to younger stars, older stars typically have larger peculiar velocities, which causes an asymmetric drift and greater vertical motion. This well-known kinematic trend must cause an age bias in kinematically selected samples.

4.1. Possible selection effects

In this work, we apply kinematic and vertical motion cuts to eliminate most thick disk and halo stars, which may well also eliminate some old thin disk stars that should perhaps be included in our samples. However, any bias in our analysis created by excluding older stars because of their higher peculiar velocities will cause lower temperature bins, which are the only bins to include stars of the old disk, to have unrepresentatively few older disk stars.

Radial mixing implies that these possibly-missing stars would be members of the most well-mixed population with the lowest radial metallicity gradient, and adding significant numbers of them to the lower T_{eff} bins would only increase the trend we observe. In fact, we find that the trend of metallicity gradient with T_{eff} is little affected by limiting the vertical excursions of selected stars to either 300 pc or 500 pc, suggesting that this cut is not biasing our result. Further restricting the vertical oscillations to < 300 pc, on the other hand, does exclude a disproportionate fraction of older stars and the trend with T_{eff} is weakened, as our argument predicts. Naturally also, the number of selected stars decreases with a more severe restriction increasing the statistical uncertainty in our esti-

mate of the metallicity gradient.

We do not use any measure of chemical composition to select stars, and our sample may therefore include some stars with enhanced $[\alpha/\text{Fe}]$. Whether such abundances best characterize thick disk stars is the subject of current debate (Ivezić *et al.* 2008; Lee *et al.* 2011) while the existence of a thick disk that is distinct from the thin has been questioned (Bovy *et al.* 2011). Our study is unaffected by these questions, because we are interested only in how the metallicity gradient changes with the mean age of the stars and, provided we have excluded halo stars that are little affected by spiral activity, we do not need to consider whether each star may or may not belong to a particular population. Note that Solway *et al.* (2012) have shown that mixing is only gradually weakened by increased random motion and vertical thickness.

A separate issue is that all the stars in this study are close to the Sun at the present time, and we therefore cannot include stars with home radii far from the Sun but with radial excursions that are too small to bring them into the solar neighborhood. However, provided the stars we do see have abundances that are representative of those of their T_{eff} and home radius, the omitted stars will not affect our estimate of the slope. Since we are not selecting on metallicity, there should be no bias in our slope estimates.

4.2. Comparison with other work

Casagrande *et al.* (2011) re-analysed the GCS using a revised calibration of T_{eff} and $[\text{Fe}/\text{H}]$ and new estimates of the individual stellar ages. We have tried to compare our results with theirs, which is not straightforward because our bins of T_{eff} each contain stars having a broad range of ages. We have used isochrone tables (Demarque *et al.* 2004) to estimate the main-sequence lifetimes of the individual stars in the GCS sample, using the T_{eff} and $[\text{Fe}/\text{H}]$ of each, and so find the average main-sequence lifetime of the stars in our separate T_{eff} bins. The mean maximum age of stars defined in this way increases from about 2 Gyr for our hottest bin to 10 Gyr for the coolest. Using these mean maximum ages to replot the trend of metallicity gradient in our Fig. 8, we find reasonable agreement with the gradient values as a cumulative function of age shown in Fig. 18(d) of Casagrande *et al.* (2011).

Our estimated gradient is in the range of other measurements from stars. For example, Coşkunoğlu *et al.* (2011) derived a metallicity gradient of -0.051 dex kpc^{-1} for F-dwarfs, and they also find a shallower gradient for the slightly older G-dwarfs. While their sample clearly overlaps with ours, they adopted different selection criteria and employed a different technique to determine the home radii, it is encouraging that they reached similar conclusions. Using disk Cepheids, which are young objects, Luck *et al.* (2011) derived $[\text{Fe}/\text{H}] = -0.055R + 0.475$, where R is the Galacto-centric radius, again in tolerable agreement with our gradient estimate for the hotter stars.

Chen *et al.* (2003) estimate a radial gradient of $[\text{Fe}/\text{H}]$ of -0.063 ± 0.008 dex kpc^{-1} from 118 star clusters. Both they and Friel *et al.* (2002) report that, when the clusters are divided by age, the slope appears steeper for the older sample, which is the opposite of our finding here. Note that the radial distribution of star clusters in these papers extends outwards from the solar radius, whereas

our sample of stars overlaps the solar radius and extends inwards to ~ 5 kpc – thus the different variations with age could indicate the absence of mixing in the outer disk. However, other systematic differences may complicate this interpretation; *e.g.*, the outer disk open clusters in the sample assembled by Chen *et al.* (2003) are farther from the mid-plane than are those near the solar radius.

Maciel *et al.* (2006) also claim a steeper abundance gradient for older planetary nebulae, although their estimated gradients for the different elements show a lot of scatter and ages are less reliable than for star clusters. It should be noted that Stanghellini & Haywood (2010) reached the opposite conclusion finding, for a sample of PNe concentrated over the radial range $3 < R < 12$ kpc, a shallower abundance gradient for the older PNe, which is in better agreement with our results.

5. CONCLUSIONS

We have used samples of local thin-disk, main-sequence stars grouped by effective temperature to demonstrate that the radial abundance gradient in the disk of the Milky Way flattens as the T_{eff} of the stars in the sample decreases. We eliminate the blurring effect of epicyclic motion by estimating the angular momentum, L_z , of each star about the center of the Galaxy, since the home, or guiding center, radius of a star is determined only by its angular momentum. Although the stars in our sample are all within 500 pc of the Sun, their home radii are spread over a wide swath of the Milky Way disk.

We interpret T_{eff} as a proxy for mean age, and conclude that a shallower gradient for stars of a greater mean age. We find some evidence that the trend of decreasing metallicity gradient with increasing age breaks to a flat trend around $5500 \lesssim T_{\text{eff}} \lesssim 6000$ K, for which the main-sequence lifetime of a star is approximately 10 Gyr, or roughly the age of the thin disk. Flattening of the metallicity gradient is consistent with the predictions of radial mixing, or churning, due to spiral patterns in the disk.

We thank Birgitta Nordström for helpful correspondence about the apparently metal rich stars in the GCS and an anonymous referee for comments that have helped us to improve the paper. This work was supported by NSF grant AST 09-37523 (PI Newberg), and grant 11061120454 (PI Deng) from the National Science Foundation of China (NSFC), the NSFC grants 11073038 (PI Chen), 11173044 (PI Hou), Key Project 10833005 (PI Hou), and by the Group Innovation Project No. 10821302.

REFERENCES

Aumer, M. & Binney, J. J. 2009, MNRAS, **397**, 1286
 Balser, D. S., Rood, R. T., Bania, T. M. & Anderson, L. D. 2011, ApJ, **738**, 27
 Bensby, T., Feltzing, S. & Lundström, I. 2003, A&A, **410**, 527
 Binney, J. & Tremaine, S. 2008, *Galactic Dynamics* 2nd Ed. (Princeton: Princeton University Press)
 Bird, J. C., Kazantzidis, S. & Weinberg, D. H. 2012, MNRAS, **420**, 913
 Breddels, M. A., Smith, M. C., Helmi, A., *et al.* 2010, A&A, **511**, A90
 Boissier, S. & Prantzos, N. 1999, MNRAS, **307**, 857
 Bovy, J., Rix, H-W. & Hogg, D. W. 2011, arXiv:1111.6585

Casagrande, L., Schönrich, R., Asplund, M., *et al.* 2011, A&A, **530**, A138
 Chen, L., Hou, J. L. & Wang, J. J. 2003, AJ, **125**, 1397
 Chiappini, C., Matteucci, F. & Romano, D. 2001, ApJ, **554**, 1044
 Coşkunoglu, B., Ak, S., Bilir, S., *et al.* 2011, MNRAS, in press
 de Jong, R. S. 1996, A&A, **313**, 377
 Demarque, P., Woo, J-H., Kim, Y-C. & Yi, S. K. 2004, ApJS, **155**, 667
 Edvardsson, B., Andersen, B., Gustafsson, B., *et al.* 1993, A&A, **275**, 101
 Friel, E. D., Janes, K. A., Tavares, M., *et al.* 2002, AJ, **124**, 2693
 Fu, J., Hou, J. L., Yin, J. & Chang, R. X. 2009, ApJ, **696**, 668
 Haywood, M. 2008, MNRAS, **388**, 1175
 Hou, J. L., Prantzos, N. & Boissier, S. 2000, A&A, **362**, 921
 Girard, T. M., van Altena, W. F., Zacharias, N., *et al.* 2011, AJ, **142**, 15
 Høg, E., Fabricius, C., Makarov, V. V., *et al.* 2000, A&A, **355**, L27
 Hollander, M. & Wolfe, D. A. 1999, *Nonparametric Statistical Methods* 2nd Ed. (New York: John Wiley) pp. 416–423
 Holmberg, J., Nordström, B. & Andersen, J. 2007, A&A, **475**, 519
 Holmberg, J., Nordström, B. & Andersen, J. 2009, A&A, **501**, 941
 Ivezić, Ž., Sesar, B., Jurić, M., *et al.* 2008, ApJ, **684**, 287
 Johnson, D. R. H. & Soderblom, D. R. 1987, AJ, **93**, 864
 Lee, Y. S., Beers, T. C., Sivarani, T., *et al.* 2008, AJ, **136**, 2022
 Lee, Y. S., Beers, T. C., An, D., *et al.* 2011, ApJ, **738**, 187
 Loebman, S. R., Roškar, R., Debattista, V. P., *et al.* 2011, ApJ, **737**, 8
 Luck, R. E., Andrievsky, S. M., Kovtyukh, V. V., *et al.* 2011, AJ, **142**, 51
 Maciel, W. J., Lago, L. G. & Costa, R. D. D. 2006, A&A, **453**, 587
 Maciel, W. J., Quireza, C. & Costa, R. D. D. 2007, A&A, **463**, L13
 Minchev, I., Famaey, B., Combes, F., *et al.* 2011, A&A, **527A**, 147
 Muñoz-Mateos, J. C., Gil de Paz, A., Boissier, S., 2007, ApJ, **658**, 1006
 Munn, J. A., Monet, D. G., Levine, S. E., *et al.* 2004, AJ, **127**, 3034
 Munn, J. A., Monet, D. G., Levine, S. E., *et al.* 2008, AJ, **136**, 895
 Naab, T. & Ostriker, J. P. 2006, MNRAS, **366**, 899
 Nordström, B., Mayor, M., Andersen, J., *et al.* 2004, A&A, **418**, 989
 Piatek, S., Pryor, C., Olszewski, E. W., *et al.* 2002, AJ, **124**, 3198
 Reid, I. N., Turner, E. L., Turnbull, M. C., *et al.* 2007, ApJ, **665**, 767
 Reylé, C., Rajpurohit, A. S., Schultheis, M. & Allard, F. 2011, arXiv:1102.1263
 Roškar, R., Debattista, V. P., Quinn, T. R., *et al.* 2008a, ApJL, **684**, L79
 Roškar, R., Debattista, V. P., Stinson, G. S., *et al.* 2008b, ApJL, **675**, L65
 Schlesinger, K. J., Johnson, J. A., Rockosi, C. M., *et al.* 2011, ApJ, submitted (arXiv:1112.2214)
 Schönrich, R. & Binney, J. 2009, MNRAS, **396**, 203
 Schönrich, R., Binney, J. & Dehnen, W. 2010, MNRAS, **403**, 829
 Sellwood, J. A. & Binney, J. J. 2002, MNRAS, **336**, 785
 Shaver, P. A., McGee, R. X., Newton, L. M., 1983, MNRAS, **204**, 53
 Siebert, A., Williams, M. E. K., Siviero, A., *et al.* 2011, AJ, **141**, 187
 Soderblom, D. R. 2010, ARAA, **48**, 581
 Solway, M., Sellwood, J. A. & Schönrich, R. 2010, MNRAS, *to appear* (arXiv:1202.1418)
 Stanghellini, L. & Haywood, M. 2010, ApJ, **714**, 1096
 Steinmetz, M., Zwitter, T., Siebert, A., *et al.* 2006, AJ, **132**, 1645
 van Leeuwen, F. 2007, A&A, **474**, 653
 West, A. A., Morgan, D. P., Bochanski, J. J., *et al.* 2011, AJ, **141**, 97
 Woolf, V. M., Lépine, S. & Wallerstein, G. 2009, PASP, **121**, 117
 Wielen, R. 1977, A&A, **60**, 263
 Yanny, B., Rockosi, C., Newberg, H. J., *et al.* 2009, AJ, **137**, 4377
 York, D. G., Adelman, J., Anderson, J. E., *et al.* 2000, AJ, **120**, 1579
 Zwitter, T., Siebert, A., Munari, U., *et al.* 2008, AJ, **136**, 421
 Zwitter, T., Matijević, G., Breddels, M. A., *et al.* 2010, A&A, **522**, A54